Electronic structure of dynamically two-dimensional hole gas in AlGaN/GaN heterostructures

2002 J. Phys.: Condens. Matter 14 3435

(http://iopscience.iop.org/0953-8984/14/13/303)

INSTITUTE OF PHYSICS PUBLISHING JOURNAL OF PHYSICS: CONDENSED MATTER

J. Phys.: Condens. Matter **14** (2002) 3435–3443 PII: S0953-8984(02)26784-3

Electronic structure of dynamically two-dimensional hole gas in AlGaN/GaN heterostructures

Agustinus Sutandi[1], **P Paul Ruden**[1] **and Kevin F Brennan**[2]

[1] Department of Electrical and Computer Engineering, University of Minnesota, Minneapolis, MN 55455, USA
[2] School of Electrical and Computer Engineering, Georgia Tech, Atlanta, GA 30332, USA

Received 11 July 2001
Published 22 March 2002
Online at stacks.iop.org/JPhysCM/14/3435

Abstract

The electronic structure of a quasi-two-dimensional hole gas near the interface of an AlGaN/GaN heterostructure is examined by calculating the valence band structure in the channel region in the framework of a six-band Rashba–Sheka–Pikus (RSP) Hamiltonian. Self-consistency in the Hartree approximation is achieved. Strain effects are included through deformation potentials and through the modulation of interfacial polarization charges associated with the piezoelectric nature of the constituent materials. It is found that for hole concentrations of 10^{13} cm^{-2}, four subbands are partially populated. The effects of externally applied stress are then considered for the two distinct cases of hydrostatic stress and uniaxial stress applied parallel to the interface. While hydrostatic stress of practical magnitude appears to modulate the electronic structure only slightly, symmetry lowering uniaxial stress leads to significant changes in the population of the subbands and large dispersion anisotropies that should be detectable in piezo-mobility studies.

1. Introduction

Group III-nitride semiconductors have become the materials of choice for optoelectronic devices operating in the short-wavelength-visible and ultraviolet bands. In addition, these materials show considerable promise for the fabrication of high-frequency, high-power electronic devices and perhaps for sensors that operate in caustic environments. One of the distinguishing features of the system of materials that is comprised of GaN, AlN, InN and their alloys, is its suitability for the growth of epitaxial heterostructures, such as those needed for heterostructure lasers and heterostructure transistors [1].

While all III-nitride materials of interest appear to have the wurtzite crystal structure (point group symmetry C_{6v}) in their most stable modification, the lattice constants vary from one binary compound to another and, hence, with alloy composition. Consequently, epitaxial heterostructures composed of these materials include layers with built-in strain. If

the heterointerfaces are perpendicular to the principal (hexagonal) crystal axis, the built-in biaxial strain does not lower the crystal symmetry.

Residual biaxial strain may be present throughout the epitaxial structure due to the fact that the III-nitrides are typically grown on foreign substrates. The most popular substrate at present is sapphire, cut perpendicular to its principal symmetry axis. Although that is only a three-fold axis (the sapphire point group symmetry is C_{3v}), the hexagonal axis of the III-nitride epilayers aligns with it. However, the crystal axes in the basal plane are rotated by $\pi/6$.

In this paper, the focus is on p-type $Al_xGa_{1-x}N$/GaN heterostructures grown along the principal crystal axis. To facilitate the formation of a two-dimensional charge carrier gas at the interface, it is helpful to exploit the polarization charge at the interface. This polarization charge is positive for $Al_xGa_{1-x}N$ on GaN structures that are grown parallel to the [0 0 0 1] direction and, hence, leads to a two-dimensional electron gas (2-DEG) [2]. The formation of a two-dimensional hole gas (2-DHG) is facilitated by a negative polarization charge at the interface. This implies a [0 0 0 $\bar{1}$] growth direction for an $Al_xGa_{1-x}N$ on GaN structure, or a so-called inverted structure (GaN on $Al_xGa_{1-x}N$) grown along [0 0 0 1]. The former case is somewhat preferable because the built-in strain of an $Al_xGa_{1-x}N$ layer grown on relaxed GaN tends to increase the magnitude of the polarization charge, while a strained GaN layer grown on unstrained $Al_xGa_{1-x}N$ yields a smaller polarization charge [3]. In the following, a structure consisting of $Al_xGa_{1-x}N$ grown pseudomorphically on GaN along the [0 0 0 $\bar{1}$] direction is assumed. However, the qualitative results obtained also apply to the inverted structure that (in modified form, with a strained $Al_xGa_{1-x}N$ layer) has recently been fabricated successfully [4].

The physics of bulk wurtzite-structure III-nitride materials and of III-nitride heterostructures includes many properties that can be modulated by the application of stress. In particular, stress affects the electronic properties of III-nitride heterostructures in multiple ways. First, the bulk bands may shift due to a deformation potential coupling between the stress-induced deformation and the electron bands. Second, polarization charges at heterointerfaces are modulated by stress through piezoelectric effects. Third, bound levels in the band gap associated with point defects, interface and surface states may shift and consequently change their charge state. Because of the complexity of the valence bands, p-type III-nitride material and heterostructures are expected to display a rich variety of piezo-resistive and piezo-optic effects. In this paper, we focus on the effects of hydrostatic and in-plane uniaxial stress on the 2-DHG formed in $Al_xGa_{1-x}N$/GaN heterostructures grown along the hexagonal axis on sapphire substrates.

2. Calculation of the 2-DHG subband structure

The calculations reported here are based on a description of the bulk valence bands near the Γ-point through a six-band Rashba–Sheka–Pikus (RSP) Hamiltonian [5]. At the Γ-point the eigenvalues of this Hamiltonian are two-fold degenerate and eigenfunctions have symmetries Γ_9, Γ_7 and Γ_7. Applied to the heterostructure problem (with z designating the direction perpendicular to the interface and parallel to the main crystal axis), the RSP Hamiltonian yields six, coupled, ordinary differential equations,

$$\begin{pmatrix} \hat{F} & 0 & -\hat{H}^* & 0 & K^* & 0 \\ 0 & \hat{G} & \sqrt{2}\Delta_3 & -\hat{H}^* & 0 & K^* \\ -\hat{H} & \sqrt{2}\Delta_3 & \hat{\lambda} & 0 & \hat{I}^* & 0 \\ 0 & -\hat{H} & 0 & \hat{\lambda} & \sqrt{2}\Delta_3 & \hat{I}^* \\ K & 0 & \hat{I} & \sqrt{2}\Delta_3 & \hat{G} & 0 \\ 0 & K & 0 & \hat{I} & 0 & \hat{F} \end{pmatrix} \begin{pmatrix} \psi_{n,1}(k_x, k_y, z) \\ \psi_{n,2}(k_x, k_y, z) \\ \psi_{n,3}(k_x, k_y, z) \\ \psi_{n,4}(k_x, k_y, z) \\ \psi_{n,5}(k_x, k_y, z) \\ \psi_{n,6}(k_x, k_y, z) \end{pmatrix} = 0 \tag{1}$$

where

$$\hat{F} = \Delta_1 + \Delta_2 + \hat{\lambda} + \hat{\theta}$$
$$\hat{G} = \Delta_1 - \Delta_2 + \hat{\lambda} + \hat{\theta}$$
$$\hat{H} = \mathrm{i}\left(A_6 \frac{1}{\mathrm{i}} \frac{\partial}{\partial z} + \mathrm{i}A_7\right)(k_x + \mathrm{i}k_y) + \mathrm{i}D_6(\varepsilon_{zx} + \mathrm{i}\varepsilon_{yz})$$
$$\hat{I} = \mathrm{i}\left(A_6 \frac{1}{\mathrm{i}} \frac{\partial}{\partial z} - \mathrm{i}A_7\right)(k_x + \mathrm{i}k_y) + \mathrm{i}D_6(\varepsilon_{zx} + \mathrm{i}\varepsilon_{yz})$$
$$K = A_5\left(k_x^2 - k_y^2 + \mathrm{i}2k_xk_y\right) + D_5(\varepsilon_{xx} - \varepsilon_{yy} + \mathrm{i}2\varepsilon_{xy})$$
$$\hat{\lambda} = -A_1 \frac{\partial^2}{\partial z^2} + A_2\left(k_x^2 + k_y^2\right) + D_1\varepsilon_{zz} + D_2(\varepsilon_{xx} + \varepsilon_{yy}) + V(z) - E_n(k_x, k_y)$$
$$\hat{\theta} = -A_3 \frac{\partial^2}{\partial z^2} + A_4\left(k_x^2 + k_y^2\right) + D_3\varepsilon_{zz} + D_4(\varepsilon_{xx} + \varepsilon_{yy}).$$

Δ_1 and $\Delta_{2,3}$ correspond to the crystal-field and spin–orbit splitting energies, respectively. A_i are the valence band parameters, corresponding to the Luttinger parameters in zinc-blende crystals. D_i are the deformation potentials for the valence bands and ε_{ij} $(i,\ j = x,\ y,\ z)$ are the components of a strain tensor, with the diagonal terms ε_{ii} positive for tension. $E_n(k_x,\ k_y)$ is the nth dynamically two-dimensional subband. $V(z)$ is the self-consistent potential that (in the Hartree approximation) consists of electrostatic contributions associated with the hole distribution and the interface polarization charge, and a contribution due to the valence band offset, ΔE_V, between $Al_xGa_{1-x}N$ and GaN, which was taken to be 0.3 of the band gap difference,

$$V(z) = V_H(z) + V_{\mathrm{pol}}(z) + \Delta E_V[\theta(z - z_{\mathrm{interface}})]. \tag{2}$$

Here $z_{\mathrm{interface}}$ designates the location of the $Al_xGa_{1-x}N$/GaN interface and $\theta(z)$ is a unit step function. Designating ε and q to represent the material permittivity and the electron charge, respectively, the polarization charge contribution to the potential is given by

$$\frac{1}{q}\frac{\mathrm{d}^2}{\mathrm{d}z^2}V_{\mathrm{pol}}(z) = -\frac{\rho_{\mathrm{pol}}(z)}{\varepsilon} \tag{3}$$

where $\rho_{\mathrm{pol}}(z) = \sigma_{\mathrm{pol}}\delta(z - z_{\mathrm{interface}})$ and σ_{pol} originates from the differences in spontaneous and piezoelectric polarization in the $Al_xGa_{1-x}N$ and GaN layers. In the absence of applied stress, we assume that the GaN layer is relaxed and that the pseudomorphic $Al_xGa_{1-x}N$ layer is biaxially dilated. The strain tensor associated with built-in strain is diagonal with $\varepsilon_{xx} = \varepsilon_{yy}$ and $\varepsilon_{zz} = -2(C_{13}/C_{33})\varepsilon_{xx}$, where C_{13} and C_{33} are the relevant elastic constants. The polarization parameters used are from [3] and are listed in table 1. Neglecting image potential effects associated with the small difference between the dielectric constants of

Table 1. Polarization parameters. P_{SP} is the spontaneous polarization and e_{ij} are piezoelectric constants.

	P_{SP} (C m^{-2})	e_{31} (C m^{-2})	e_{33} (C m^{-2})
AlN	−0.081	−0.60	1.46
GaN	−0.029	−0.49	0.73

$Al_xGa_{1-x}N$ and GaN, the Hartree potential associated with the holes in the valence band is given by

$$\frac{1}{q}\frac{\mathrm{d}^2}{\mathrm{d}z^2}V_H(z) = -\frac{\rho_{2\text{-DHG}}(z)}{\varepsilon} \tag{4}$$

with

$$\rho_{2\text{-DHG}}(z) = \frac{q}{(2\pi)^2}\iint \sum_n \sum_{\nu=1}^{6} |\psi_{n,\nu}(k_x, k_y, z)|^2 \,\mathrm{d}k_x \,\mathrm{d}k_y. \tag{5}$$

The summations over subbands, n, and the two-dimensional k-space integration extend over filled states only.

The band dispersions have circular symmetry in the (k_x, k_y)-plane and the envelope wavefunctions, $|\psi_{n,\nu}(k_x, k_y, z)|^2$ $(\nu = 1, \ldots, 6)$, for the valence band states depend only on $k_\parallel = \left(k_x^2 + k_y^2\right)^{1/2}$. This symmetry reduces the two-dimensional integration in equation (5), to a one-dimensional integration,

$$\rho_{2\text{-DHG}}(z) = \frac{q}{(2\pi)^2} 2\pi \int k_\parallel \sum_n \sum_{\nu=1}^{6} |\psi_{n,\nu}(k_\parallel, z)|^2 \,\mathrm{d}k_\parallel. \tag{6}$$

A non-uniform discretization of the $k_\parallel$-axis, so as to ensure equal hole density increments, is implemented to facilitate the self-consistent determination of filled states, which is done based on zero temperature Fermi–Dirac statistics.

The problem given by equation (1) is solved by a finite difference method. The code is parallelized so that the coupled difference equations are solved for up to 24 k-points simultaneously [6][3]. The RSP Hamiltonian parameters used are from [7, 8] and are listed in tables 2 and 3. Because of the current uncertainty in the A_i-parameters, no distinction between those of the $Al_xGa_{1-x}N$ alloy and those of GaN was made. However, since the crystal-field splitting parameters, Δ_1, of GaN and AlN differ considerably, this variation was taken into account. All alloy parameters were linearly interpolated from the binary compound values.

Table 2. RSP Hamiltonian parameters. Δ_i are in meV; A_i $(i = 1, 2, \ldots, 6)$ are in units of $\frac{1}{2}\left(\hbar^2/m_e\right)$ where m_e is the free electron rest mass; A_7 is in meV Å.

Δ_1	Δ_2	Δ_3	A_1	A_2	A_3	A_4	A_5	A_6	A_7
21.1 (GaN) −215 (AlN)	3.61	3.61	−7.21	−0.440	6.68	−3.46	−3.40	−4.9	93.7

Table 3. Deformation potentials for GaN.

D_1 (eV)	D_2 (eV)	D_3 (eV)	D_4 (eV)	D_5 (eV)
−13.87	−13.71	2.92	−1.56	−2.05

[3] Alternatively the problem may be solved by a spectral method as was done for the preliminary results reported in [6].

As pointed out above, in addition to built-in strain due to lattice mismatch, strain may be created through the application of external stress. Several distinct stress geometries are of current interest because of the relative ease with which the corresponding experiments may be performed [9]. Hydrostatic stress is expected to cause band shifts, but it leaves the symmetry of the III–nitride epilayer structure unperturbed. Similarly, uniaxial stress applied along the hexagonal axis causes quantitative changes but preserves the symmetry. However, uniaxial stress in the basal plane, i.e. in the plane of the substrate, reduces the symmetry from C_{6v} to C_{2v}.

In the case of uniaxial stress within the basal plane, the symmetry is lowered and the subbands and envelope wavefunctions are dependent on $k_{x'}$ and $k_{y'}$, which are conveniently chosen to be parallel to and perpendicular to the stress axis, respectively. For the calculation of the self-consistent potential, however, the consequences of the symmetry lowering are found to be small. Hence, the one-dimensional $k_\parallel$ integral can still be used if an effective $k_\parallel$-axis (intermediate between $k_{x'}$ and $k_{y'}$) is selected so as to ensure that the Fermi energy is approximately unaffected. To this end the effective $k_\parallel$-axis used in the integration, equation (6), is determined from,

$$\frac{\cos^2\varphi}{m^*_{0,x'}} + \frac{\sin^2\varphi}{m^*_{0,y'}} = \frac{1}{\sqrt{m^*_{0,x'}m^*_{0,y'}}} \rightarrow \varphi = \arccos\left(\sqrt{\frac{\sqrt{m^*_{0,x'}m^*_{0,y'}} - m^*_{0,x'}}{m^*_{0,y'} - m^*_{0,x'}}}\right) \tag{7}$$

where $m^*_{0,x'}$ is the hole effective mass of the lowest (most populated) subband along the stress direction and $m^*_{0,y'}$ is the corresponding hole effective mass in the direction perpendicular to the stress axis; φ designates the angle of the effective $k_\parallel$-axis and $k_{x'}$.

The strain tensor elements in equation (1) are evaluated in linear elastic theory based on the elastic constants of GaN [10] and sapphire [11]. We assume that the overall elastic response of the sample consisting of a thick sapphire substrate and a relatively thin III-nitride overlayer is primarily determined by the stiffness of the sapphire and that any in-plane stress on the sapphire/III-nitride interface is transferred to the epitaxial structure. In considering uniaxial stress, the stress is applied to the sapphire substrate in the basal plane along the principal in-plane crystal axis. The resulting strain tensor in the III-nitride material has non-zero off-diagonal elements ε_{xy}, in addition to three different diagonal elements, $\varepsilon_{xx} \neq \varepsilon_{yy} \neq \varepsilon_{zz}$. The remaining strain tensor elements vanish. Variations of the polarization charge at the interface with stress arise from the differences in the piezoelectric parameters of the $Al_xGa_{1-x}N$ and GaN.

3. Results and discussion

In this section we present results for two different two-dimensional hole concentrations. Experimentally the equilibrium hole concentration will depend on several parameters that do not enter the calculations performed for this work. Among these parameters are the thickness of the $Al_xGa_{1-x}N$ layer, the doping profile in the structure and the surface potential, which itself may be controlled by an applied potential, if a suitable conducting gate layer is deposited onto the $Al_xGa_{1-x}N$ layer.

Figure 1 displays calculated results for the top of the valence band in a p-type $Al_{0.25}Ga_{0.75}N$/GaN heterostructure without applied stress. The interface polarization charge density is $-1.41 \times 10^{13}\ q\ \mathrm{cm}^{-2}$, and the assumed two-dimensional hole gas density is $5 \times 10^{12}\ \mathrm{cm}^{-2}$. Figure 1(a) shows the bulk band profile along the z-direction, together with the ($T = 0$) Fermi level and the lowest hole energy subband levels, which are doubly degenerate at $k_\parallel = 0$. The lowest four hole energy subbands are partially occupied. Also shown is the hole

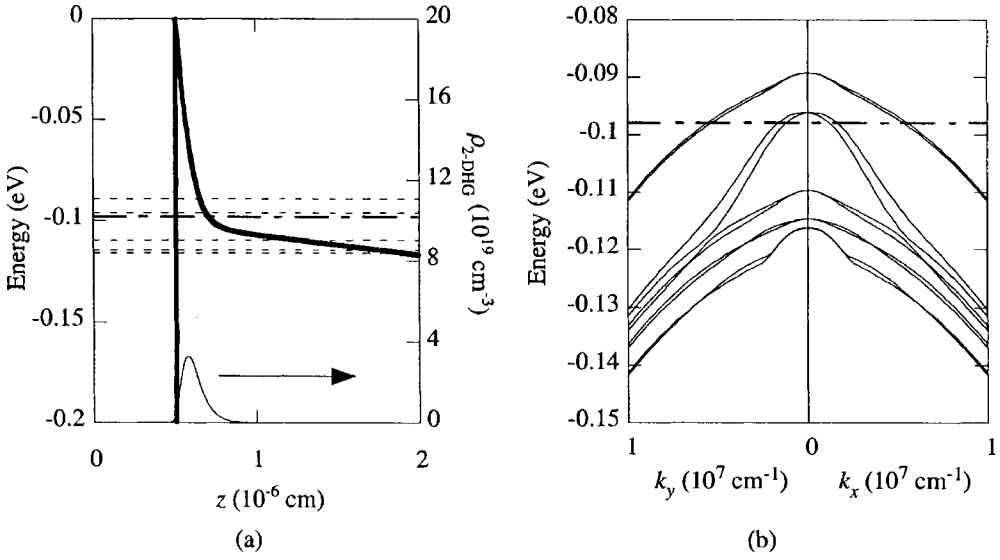

Figure 1. Valence band profile (a), and subband dispersion (b), for an $Al_{0.25}Ga_{0.75}N/GaN$ heterostructure with no external stress applied and 2-DHG concentration of $5 \times 10^{12}\,cm^{-2}$. In (a), the dashed lines represent the $k_\parallel = 0$ subband levels. Also shown is the hole distribution perpendicular to the interface. In (a) and (b), the long-short-long dashed line represents the Fermi level.

density profile as determined from equation (6). Figure 1(b) illustrates the band dispersion in the plane of the interface. As is clearly seen, the bands are far from parabolic and tend to anticross due to the coupling between different bands that is described by the off-diagonal terms in equation (1). However, the bands have circular symmetry. Very apparent (in figure 1(b)) is the spin splitting of the third and fourth subbands. This originates from the lack of inversion symmetry that, in conjunction with the spin–orbit interaction, manifests itself through the linear A_7 term in the bulk RSP Hamiltonian and through the non-symmetric potential $V(z)$. In fact, performing the calculation with $A_7 = 0$ is found to lead to a spin splitting of comparable magnitude to the one shown in figure 1(b), in sharp contrast to the situation encountered in symmetric quantum well structures [8, 12, 13]. At $k_\parallel = 0$, all levels are two-fold spin-degenerate and, suppressing a spin index, the associated states may be classified according to symmetry as $(\Gamma_n)_m$, where $n = 7$ or 9 and $m = 0, 1, 2, \ldots$ is an index given by the number of nodes of the envelope function. In order of increasing hole energy, the states are then labelled as: $(\Gamma_9)_0$, $(\Gamma_7)_0$, $(\Gamma_9)_1$, $(\Gamma_9)_2$, and $(\Gamma_7)_1$. Figures 2(a) and (b) show the results obtained with a hole concentration of $10^{13}\,cm^{-2}$. Again, the lowest four subbands are partially populated.

Next, the effect of applying 20 kbar of hydrostatic pressure was examined. Although the strain components are appreciably large, the interface polarization charge density increases in magnitude by a modest 2.2% relative to the case without applied stress. The deformation potential terms give rise to slight shifts (on the order of meV) in the subband structure, but these are essentially invisible on the scale of the figures shown here, and, for brevity, results for hydrostatic stress are therefore not reproduced in this paper.

The case of in-plane uniaxial stress, on the other hand, is readily appreciated. Figures 3 and 4 illustrate the effect of 20 kbar of uniaxial stress applied to the structure, parallel to the principal crystal axis in the basal plane of the sapphire. Figures 3 and 4 show the results for hole

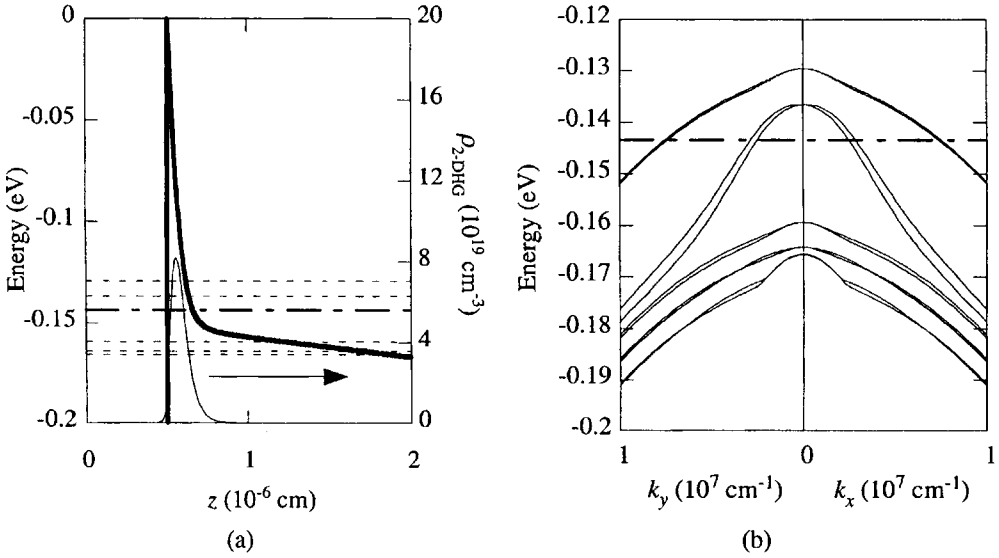

Figure 2. Valence band profile (a), and subband dispersion (b), for an $Al_{0.25}Ga_{0.75}N/GaN$ heterostructure with no external stress applied and 2-DHG concentration of 10^{13} cm^{-2}. In (a), the dashed lines represent the $k_\parallel = 0$ subband levels. Also shown is the hole distribution perpendicular to the interface. In (a) and (b), the long-short-long dashed line represents the Fermi level.

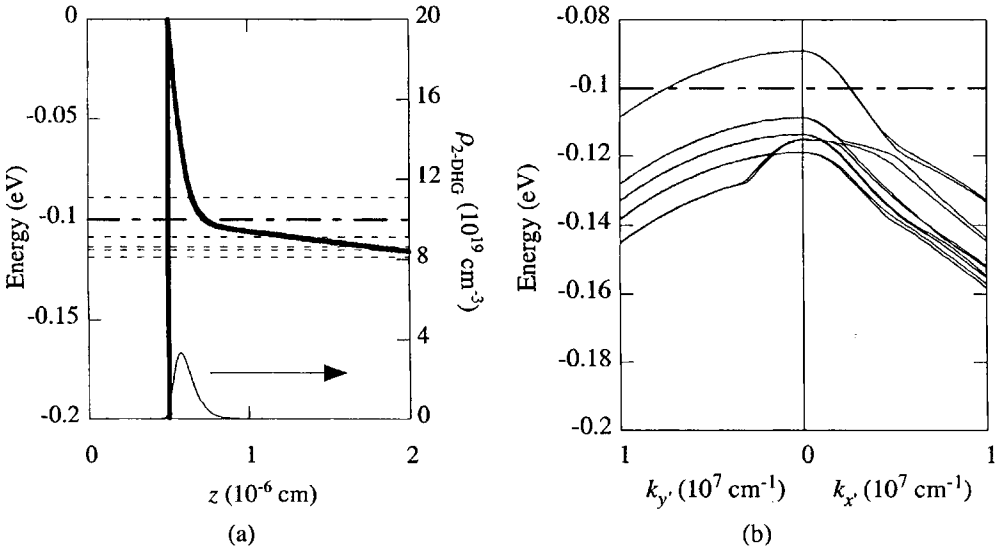

Figure 3. Valence band profile (a), and subband dispersion (b), for an $Al_{0.25}Ga_{0.75}N/GaN$ heterostructure with 20 kbar of externally applied compressive uniaxial stress along the x' direction and 2-DHG concentration of 5×10^{12} cm^{-2}.

concentrations of 5×10^{12} cm^{-2} and 10^{13} cm^{-2}, respectively. The interface polarization charge density again varies only modestly, decreasing by 1.3% in magnitude relative to the unstressed case. Clearly, there is considerable redistribution of the 2-DHG within the subband structure. While in the unstressed case the holes populate the lowest four subbands, in the stressed

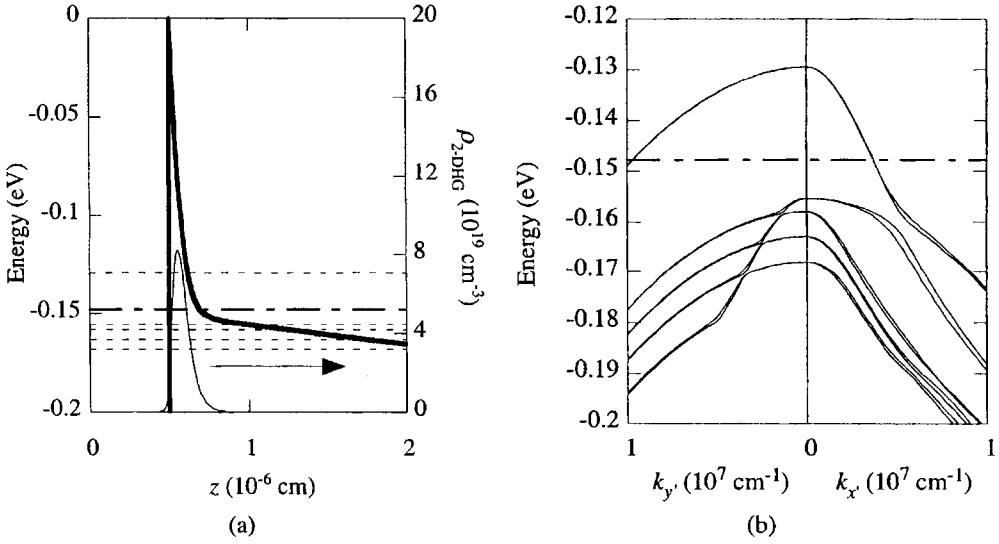

Figure 4. Valence band profile (a), and subband dispersion (b), for an $Al_{0.25}Ga_{0.75}N/GaN$ heterostructure with 20 kbar of externally applied compressive uniaxial stress along the x' direction and 2-DHG concentration of 10^{13} cm^{-2}.

situation only two subbands are partially occupied. At $k_\parallel = 0$, the symmetries of the two-fold degenerate states in order of increasing hole energy are $(\Gamma_9)_0$, $(\Gamma_9)_1$, $(\Gamma_9)_2$, $(\Gamma_7)_0$ and $(\Gamma_9)_3$, for the case shown in figure 3, and $(\Gamma_9)_0$, $(\Gamma_7)_0$, $(\Gamma_9)_1$, $(\Gamma_9)_2$ and $(\Gamma_9)_3$, for the larger hole concentration of figure 4. Furthermore, the stress leads to pronounced anisotropy in the subband dispersion such that the average effective masses of the holes differ by a factor greater than five for the directions parallel to and perpendicular to the stress axis.

Several approximations made in the calculations reported in this work merit closer examination. We neglected the differences between the valence band parameters of $Al_xGa_{1-x}N$ and GaN (with the exception of the crystal-field splitting), and any differences between the cell-periodic parts of the bulk crystal wavefunctions. It has recently been pointed out that a more rigorous calculation may be based on a symmetrized Hamiltonian [13]. However, we feel that, given the present uncertainty in the bulk valence band parameters of AlN and, in particular, of the $Al_xGa_{1-x}N$ alloy, our practice is a reasonable first approximation.

Potentially more serious is our use of the (static) Hartree approximation. Examining the hole density profiles calculated, one finds that the r_s-parameter (the mean distance between holes in units of the effective Bohr radius) can be significantly greater than unity. This indicates that exchange and correlation effects could change some of the quantitative results presented here, as recently shown for $Al_xGa_{1-x}N/GaN$ quantum wells composed of zincblende phase III-nitrides [14]. An investigation of exchange and correlation effects in the wurtzite structure system studied here is currently in progress.

Finally, in comparing stressed and unstressed structures we have taken the two-dimensional hole concentration to be constant. This may be achieved in a gated structure where a suitable variation of the applied surface (gate) potential may compensate for any stress-induced variation of the equilibrium hole density. The latter may arise from a variety of mechanisms. As noted, the interface polarization charge density is modulated even by uniform strain because the piezoelectric constants of GaN and $Al_xGa_{1-x}N$ differ. For the example discussed here, however, this amounts only to changes on the order of a few per cent.

However, energy shifts of surface and bulk defect states may also affect the hole concentration, as reported for electron channel $Al_xGa_{1-x}N/GaN$ heterostructures [15]. Because of the present lack of information on the stress dependence of defect states in this material system, a calculation of the hole density as a function of stress is beyond the scope of this work.

4. Conclusions

We report calculations of the dynamically two-dimensional subband structure of holes at a wurtzite phase AlGaN/GaN interface. The band calculations based on the RSP Hamiltonian are self-consistent in the Hartree approximation. The effect of externally applied stress is examined and the physics of stress effects on the valence band structure of III-nitride heterostructures is found to be quite rich. In particular we find that the case of uniaxial, in-plane stress discussed in this work gives rise to considerable anisotropy of the two-dimensional subband structure that is not present in the absence of uniaxial stress. Careful analysis of stress-dependent electrical characterization experiments may yield improved material parameters, such as deformation potentials and piezoelectric constants.

Acknowledgments

We thank M I Nathan for stimulating discussions. This work was supported in part by the National Science Foundation (ECS), by the Office of Naval Research, and by the Minnesota Supercomputing Institute for Digital Simulation and Advanced Computation.

References

[1] Gil B (ed) 1998 *Group III Nitride Semiconductor Compounds: Physics and Applications* (New York: Oxford University Press)
[2] Aktas O, Fan Z F, Botchkarev A, Mohammad S N, Roth M, Jenkins T, Kehias L and Morkoc H 1997 *IEEE Electron Device Lett.* **18** 293
[3] Ambacher O, Smart J, Shealy J R, Weimann N G, Chu K, Murphy M, Schaff W J, Eastman L F, Dimitrov R, Wittmer L, Stutzmann M, Rieger W and Hilsenbeck J 1999 *J. Appl. Phys.* **85** 3222
[4] Shur M S, Bykhovski A D, Gaska R, Yang J W, Simin G and Khan M A 2000 *Appl. Phys. Lett.* **76** 3061
[5] Bir G L and Pikus G E 1974 *Symmetry and Strain-Induced Effects in Semiconductors* (New York: Wiley)
[6] Sutandi A, Ruden P P and Brennan K F 2001 *Paper E 4.7 Mat. Res. Soc. Spring Meeting (San Francisco, CA)*
[7] Ren G B, Liu Y M and Blood P 1999 *Appl. Phys. Lett.* **74** 1117
[8] Suzuki M and Uenoyama T ed B Gil 1998 *Group III Nitride Semiconductor Compounds: Physics and Applications* (New York: Oxford University Press) p 307
[9] Fung A K, Albrecht J D, Nathan M I, Ruden P P and Shtrikman H 1998 *J. Appl. Phys.* **84** 3741
[10] Polian A, Grimsditch M and Grzegory I 1996 *J. Appl. Phys.* **79** 3343
[11] Simmons G and Wang H 1971 *Single Crystal Elastic Constants and Calculated Aggregate Properties: A Handbook* 2nd edn (Cambridge, MA: MIT Press)
[12] Sirenko Y M, Jeon J-B, Kim K W, Littlejohn M A and Stroscio M A 1996 *Appl. Phys. Lett.* **69** 2504
[13] Mireles F and Ulloa S E 1999 *Phys. Rev.* B **60** 13659
[14] Rodrigues S C P, Sipahi G M, Scolfaro L M R and Leite J R 2001 *J. Phys.: Condens. Matter* **13** 3381
[15] Fung A K, Cai C, Ruden P P, Nathan M I, Chen M, Sullivan G J, McDermott B, Van Hove J, Boutros K, Redwing J, Yang J, Chen Q, Khan M, Schaff W and Murphy M 1999 *Mat. Res. Soc. Symp.* **572** 495